D23

23

A NEW FLOW MODEL FOR HIGHLY SEPARATED AIRFOIL FLOWS AT LOW SPEEDS*

Glen W. Zumwalt
Wichita State University

Sharad N. Naik
Beech Aircraft Corporation

SUMMARY

An analytical model for separated airfoil flows is presented which is based on experimentally observed physical phenomena. These include a free stagnation point aft of the airfoil and a standing vortex in the separated region. A computer program is described which iteratively matches the outer potential flow, the airfoil turbulent boundary layer, the separated jet entrainment, mass conservation in the separated bubble, and the rear stagnation pressure. Separation location and pressure are not specified a priori. Results are presented for surface pressure coefficient and compared with experiment for three angles of attack for a GA(W)-1, 17% thick airfoil.

INTRODUCTION

Separated flow on wings has drawn researchers' interest ever since it was found to be responsible for aircraft stall. Interest has recently intensified due to the ability of the new GA(W) series of airfoils to operate stably with flow separated up to half of the upper surface length. However, research was long restricted to experimental observation due to the complexity of the phenomenon. For very low Reynolds numbers, solution of the Navier-Stokes equations should provide an analysis of the flow, but even with modern computers, this is a costly task. For realistic airfoils, turbulent flows occur and require some sort of mathematical model. Several models have been proposed and solved by computers with various simplifying assumptions or empirical relations. Most of the previously proposed models consider the separated region to extend to infinity downstream or it is modeled as a bulbous region. The actual physical processes in the separated region have not been included in the models. Although some of these methods have produced reasonably good computational results, their ranges of applications are generally limited and empirical input is usually required.

A mathematical model was sought which included the principal physical features. The model was first formulated by logic, found to conform to the velocity and pressure data, and then tested by special wind tunnel and electric ana-

*This research was supported by NASA Grant NSG 1192 and is available in more complete form in NASA CR-145249 (ref. 1).

366

PAGE INTENTIONALLY BLANK

log experiments. Finally, a computational program was devised with the objective of minimizing the empirical information required for solution. This program was used to predict pressures on an airfoil for which detailed data were available for comparison and evaluation of the model.

Symbols are defined in an appendix.

ORIGIN OF THE FLOW MODEL

A sketch of the flow model is shown in figure 1. The flow has separated from the upper surface and leaves the lower surface at the trailing edge. The jet mixing sheets starting from the two airfoil separation points coalesce to form the separation bubble behind the airfoil. These two jets entrain air from the dead air region (near-wake). The entrained air has to be replaced by backflow of air which must be supplied from somewhere. If S and S' (fig. 1) are the two separation streamlines, it can be seen that the amount and width of flow entrained are growing in the downstream direction; consequently, the space available for backflow decreases and the demand for it increases. Since this cannot continue very far, a termination is required of the near wake recirculation region, and a stagnation point is formed. At this point the two streams rejoin defining the end of the separation bubble.

The entrained masses of the two jets are not the same, since their lengths and velocities are different. Generally, the upper one will entrain a larger mass. Therefore, the stagnating streamlines are not necessarily the separating streamlines, S and S'. Figure 1 shows two other streamlines R and R' stagnating at the rear point and providing passages for the flow to enter and leave the separation bubble. The mass flow rate through the corridor between R and S must be the same as that between R' and S'. Further, R and R' do not terminate at the stagnation point but must continue upstream and downstream. Mass conservation in the region requires the formation of two vortices and an S-shaped corridor of flow from bottom to top.

At this point experimental verification was sought for this seemingly logical model. No reference could be found to a stable free vortex above the trailing edge, nor was the existence of a free stagnation point documented. At Wichita State University, wind tunnel tests were in process for the GA(W)-1 airfoil under NASA contract. Detailed measurements of pressure and velocity were made downstream of the trailing edge at high angles of attack (ref. 2). Figures 2 and 3 are typical results of these tests and can be seen to verify (a) the locally high pressure region just aft of the trailing edge and (2) the recirculating flow region terminating at the rear high pressure point.

Based on experimental data, constant pressure is assumed in the whole separated region except in the neighborhood of the stagnation point, where a locally high pressure region will form along the RR' line, turning back the low velocity flows.

Viscous effects can be ignored in the neighborhood of the rear stagnation point and all velocity changes considered as being due to the pressure gradi-

ents. Thus, the region is divided into viscous dominated and pressure dominated regions. This follows the classical approach originated by Prandtl for boundary layers and more recently applied successfully to separated and reattaching flows in the Chapman-Korst mixing models.

The trailing edge plane is assumed to divide the constant pressure region of the separated flow and the region of pressure rise to the rear stagnation point. This plane is also the location for satisfying the mass continuity.

Since the vortex was not discernible, a simple flow test was devised to determine its existence. A 25.4 cm chord GA(W)-1 airfoil was placed in a low speed tunnel with a thin aluminum "splitter" plate mounted parallel to the flow at midspan. The plate extended downstream of the airfoil about one chord length. The plate was painted or spotted with a lampblack-and-oil mixture to provide visualization of streamlines, as shown in figures 4 and 5. (Flow is right to left.) The main observations are:

(1) The wake closes behind the airfoil to form a "bubble" with a free stagnation point quite close to the trailing edge.

(2) The recirculating flow in the near wake forms a large, unsymmetrical vortex above the rear portion of the airfoil.

(3) There is an upward flow from the lower wake of the airfoil flowing upstream in the separation bubble and then around the vortex to join the main stream. This S-shaped, lower-to-upper flow was clearly seen on the streaked plates.

With a view toward making a mathematical model, an electric analog of the separated airfoil flow was set up. The electric potential of the airfoil was adjusted to meet the Kutta condition at the lower trailing edge, and an additional voltage point was placed above and aft of the trailing edge. This created the S-shaped lower-to-upper flow, a topside separation, and a rear stagnation. The streamlines around the airfoil surface were found to be sensitive to the strength of the rear potential point, but quite insensitive to the exact location. This fact was used in formulating the mathematical model.

COMPUTATION OF THE MODEL

The mathematical model consists of a potential flow, a boundary layer on the airfoil surface, and a separated flow region. These are iteratively matched, together with mass conservation requirements, to reach a solution.

Assumptions Made

1. Steady, incompressible, plane flow of air.
2. The boundary layer is fully turbulent.

3. The rear stagnation point is located downstream of the trailing edge one-third the distance between the upper separation point and the trailing edge. This was empirically derived and the solution was found to be quite insensitive to this value, as the electrical analog study suggested.

4. There is a constant-velocity reverse flow region, a "core flow" for the recirculating air, having a velocity 20% that of the adjacent free stream. Experimental evidence for the constant-velocity profile was abundant but no logical model can be suggested to give a "core flow" from the reversal of a shear flow. Therefore, a purely empirical choice was accepted as necessary and the 20% value derived from the examination of several GA(W) wing flow measurements. Results were somewhat sensitive to this choice, and this is regarded as the one genuinely empirical value in the flow model computation.

5. The streamlines which stagnate behind the body do so without loss of total pressure. This is the commonly used Chapman-Korst jet-mixing flow model. The pressure variation from the trailing edge to the stagnation point is approximated by a parabolic variation to conform to experimental trends. Results were found to be insensitive to this choice.

Potential Flow

A potential flow solution method was required which would give velocities and pressures for specified geometries on the forward and lower airfoil surfaces, and also produce streamline geometry for a specified pressure distribution in the separated regions. The Mixed Boundary Condition potential flow program of McDonnell Aircraft Company, St. Louis, met this requirement and was made available. This program is a modification of the wing-body code developed by Woodward (ref. 3). The airfoil is divided into a number of panels on the chordline and the thickness, camber and angle of attack are represented by planar sources and vortex singularities. Panel lengths chosen for computation were 1% of chord near the leading and trailing edges, and these increased 5% in the center of the airfoil. Near wake panels were also 1% long. The potential program treated the separated region as an extension of the airfoil, with the body terminating at the rear stagnation point.

Boundary Layer Analysis

Head's entrainment method (ref. 4) of calculating the turbulent boundary layer was chosen as being sufficiently accurate without undue complexity. The flow was assumed to be turbulent from the leading edge or, on the lower side, from the front stagnation point. After the potential flow solution was accomplished, the displacement thickness was computed and added to the airfoil surface. The augmented airfoil was again solved by the potential program and the process repeated to convergence. Since the potential program provided the separation streamline shape, the displacement thickness at the separation point was added to the ordinates of the separation streamline to obtain the effective displacement surface.

The criteria for separation of the boundary layer was the value of the shape factor, H, which is the ratio of the displacement thickness to the momentum thickness. Most integral methods assume H values of 1.8 to 2.4 as the separation indicator. The exact value appears to depend on surface curvature, backflow strength, and possibly the upstream boundary layer history. This value was varied in the program as a means of "ordering" the separation point to move. An initial value of 2.2 was used with separation at 95% chord.

Jet Mixing Analysis

A jet mixing computation was needed for the upper stream to permit calculation of the mass entrained. Since the model assumes, on the basis of experimental evidence, that the separated flow is at constant pressure (equal to the separation point pressure), a constant pressure mixing theory is needed. The Korst turbulent jet mixing method (ref. 5) was adapted to the incompressible case for the flow on the upper surface from separation to the rear stagnation point. The virtual origin method of Hill (ref. 6) was used to handle the effects of the initial boundary layer at separation on the jet mixing. This then produces a velocity profile at the plane of the trailing edge.

Determination of the Stagnating Streamlines

The two streamlines R and R' (see fig. 6) can be found from the two requirements (1) that their velocities are equal and (2) that the mass entering the separation bubble between R' and the lower surface must equal the mass leaving between streamlines S and R. The model assumes a constant static pressure separated region which applies to R' and R at the trailing edge plane. Their stagnation pressures are also equal, since they stagnate at the same point. Thus, their velocities must be equal. The equal mass flow requirement is performed at the trailing edge plane. A velocity value for R and R' is iterated until the mass requirement is met. A new rear stagnation point pressure results. If it differs from the value previously used, the potential flow and boundary layer must be recalculated and the new R and R' streamlines located.

Recirculating Mass Balance

The Korst error function velocity profile is used for variation from the local potential flow velocity to the reverse core flow velocity. The Goertler jet spreading parameter, σ, required for the mixing analysis, was used with the well-established incompressible value of 12. The airfoil upper surface is augmented by the displacement thickness at the lower trailing edge. This pictures the lower boundary layer as swirling almost unchanged around a small separation bubble at the trailing edge. The mass flow is integrated from the displaced upper surface of the airfoil to the S streamline in the transverse plane of the trailing edge. If the net mass flux is not zero, the value of the shape factor H for separation is changed and the entire computation process is repeated until mass conservation is reached.

COMPUTED RESULTS

Figure 7 illustrates the program logic. In this figure, P_R refers to the pressure at the rear stagnation point. This program was used to calculate the pressure distributions on the GA(W)-1 17% thick airfoil at three angles of attack (18.4°, 16.4°, and 14.4°) for which experimental data were available (ref. 7). The results are shown in figures 8, 9 and 10. It can be seen that agreement with experiment is good. The separation pressure is predicted quite accurately and the separation location is slightly aft of the experimental values. The rear stagnation pressures also agree well with experiments. Comparative values are given in Table 1.

The method does not prescribe any of the separation variables. Examination of the computational histories shows that the separation point and pressure vary freely as the iterations proceed. Accuracy is dependent upon the number of panels used. The computed pressures show deviations from experimental values at about 15% chord where panel size was increased suddenly. By choosing a larger number of panels the accuracy would be improved at the cost of increased computing time. Using 29 panels on the airfoil, computation times on an IBM 360/44 or 370/145 were 14 to 40 minutes, depending on angle of attack and iterative accuracy desired.

Some improvements are needed in the computational elements. The potential program used represented the airfoil by a singularity distribution on the chord line. This is adequate for thin airfoils, but for airfoils with large thickness or angle of attack, there can be significant errors. A potential program using surface singularities (but still of the mixed boundary layer condition type) would improve accuracy. Similarly, Head's boundary layer method is usable and simple, but is not the most accurate available. Computations should be made for other airfoils to evaluate the reverse flow velocity assumption.

However, even at this point of development, this model has been shown to include all of the significant physical features, to be capable of computation with reasonable computer times, and to give good surface pressure results.

APPENDIX

SYMBOLS

C	Chord Length
C_p	Pressure Coefficient
C_{P_R}	Pressure Coefficient at Rear Stagnation Point
H	Shape Factor of Boundary Layer
M	Mach Number
$\dot{M}$	Mass Flow Rate
P_R	Pressure at Rear Stagnation Point
R.N.	Reynolds Number Based on Airfoil Chord
R	Streamline which stagnates at rear
S	Streamline which separates from surface
X_{sep}	Length from separation point to airfoil trailing edge; fraction of chord length.
α	Angle of Attack
δ	Boundary Layer Thickness
δ^*	Boundary Layer Displacement Thickness
σ	Jet Spreading Parameter

Subscripts:

L	Lower side of airfoil
SEP	Separation point
U	Upper side of airfoil
∞	Free stream value

Superscript:

Prime indicates lower-side flow

REFERENCES

1. Zumwalt, Glen W.; and Naik, Sharad N.: An Analytical Model for Highly Separated Flow on Airfoils at Low Speeds. NASA CR-145249, 1977.

2. Seetharam, H.C.; and Wentz, W.H., Jr.: Experimental Studies of Flow Separation and Stalling on a Two-Dimensional Airfoil at Low Speeds. NASA NASA CR-2560, 1975.

3. Woodward, F.A.: Analysis and Design of Wing Body Combinations at Subsonic and Supersonic Speeds. Journal of Aircraft, Vol. 5, No. 6, Nov.-Dec., 1968.

4. Head, M.R.; and Patel, V.C.: Improved Entrainment Method for Calculating Turbulent Boundary Layer Development. British R&M 3643, March 1968.

5. Korst, H.H.: A Theory of Base Pressures in Transonic and Supersonic Flow. Journal of Applied Mechanics, Vol. 23, 1956, pp. 593-600.

6. Hill, W.G., Jr.; and Page, R.H.: Initial Development of Turbulent Compressible Free Shear Layer. ASME Paper No. 68 WA/FE-21, 1968.

7. Wentz, W.H., Jr.; and Seetharam, H.C.: The Development of a Fowler Flap System for a High Performance Subsonic Flow Analysis. NASA CR-2443, Dec. 1974.

TABLE 1.- RESULTS FROM PRESENT ANALYSIS AND EXPERIMENT (REFS. 2 AND 7)

			X_{SEP}		$C_{P_{SEP}}$		C_{P_R}		H_{SEP}	
α	M_∞	R.N.	THEORY	EXPT.	THEORY	EIPT.	THEORY	EXPT.	THEORY	EXPT.
18.4°	0.16	2.5×10^6	52%	45%	-0.583	-0.60	-0.076	no data	1.9	no data
16.4°	0.21	2.9×10^6	57%	55%	-0.496	-0.50	+0.0595	no data	1.85	no data
14.4°	0.21	2.9×10^6	65%	70%	-0.285	-0.3	+0.1602	no data	1.8	no data
18.4	0.135	2.2×10^6	44%	45%	-0.640	-0.6	-0.135	≈-0.12	1.85	1.67
14.4	0.135	2.2×10^6	60%	65%	-0.33	-0.4	0.119	≈0.0	1.80	1.81

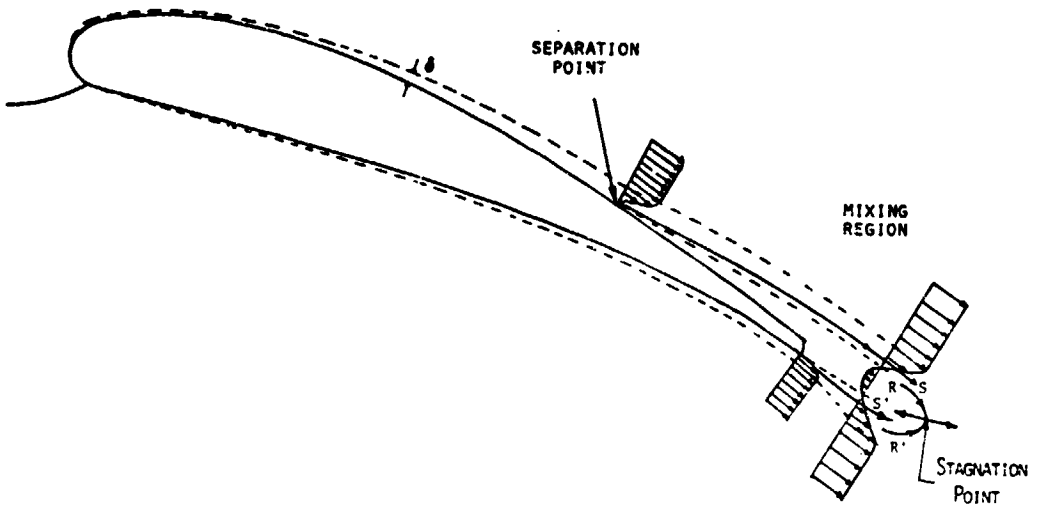

Figure 1.- Schematic diagram of separated flow model.

ALPHA =18•4 DEG•
RN = 0•222E 07
MACH NO• 0•130

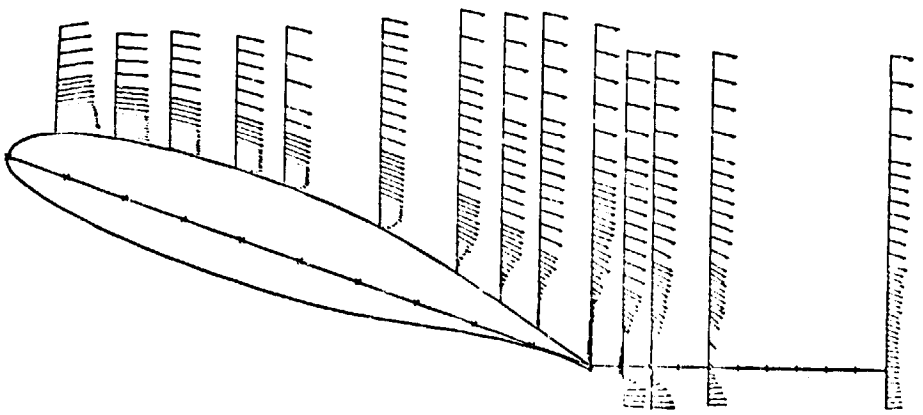

Figure 2.- Experimental velocity plot. GA(W)-1 airfoil.

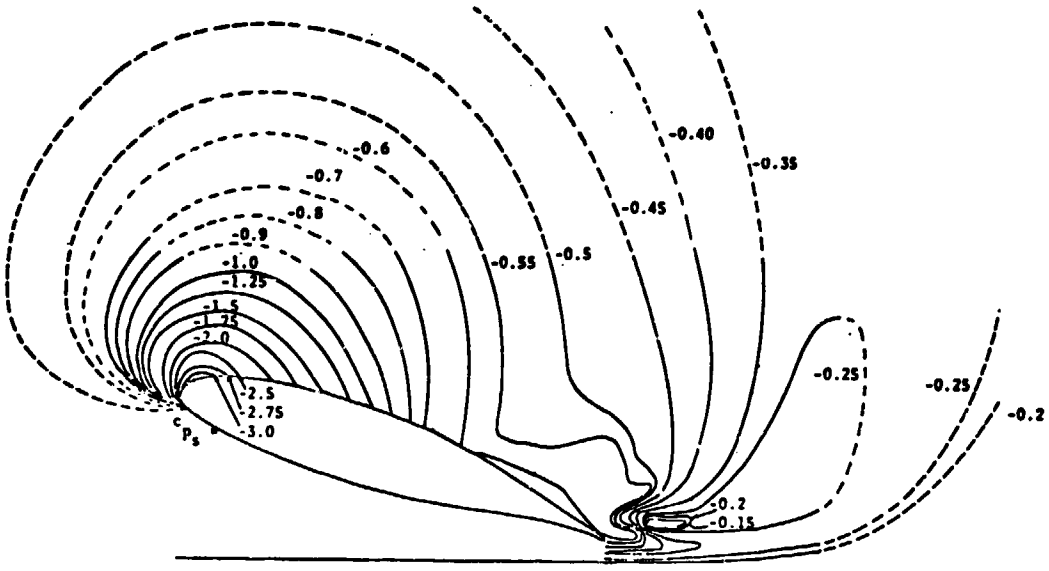

Figure 3.- Static-pressure field contours. GA(W)-1 airfoil. $\alpha = 18.4°$; R.N. = 2.2×10^6 (from ref. 2).

Figure 4.- Oil-streak flow visualization. $\alpha = 16°$; R.N. = 0.3×10^6.

Figure 5.- Oil-streak flow visualization.
$\alpha = 16°$; R.N. = 0.3×10^6.

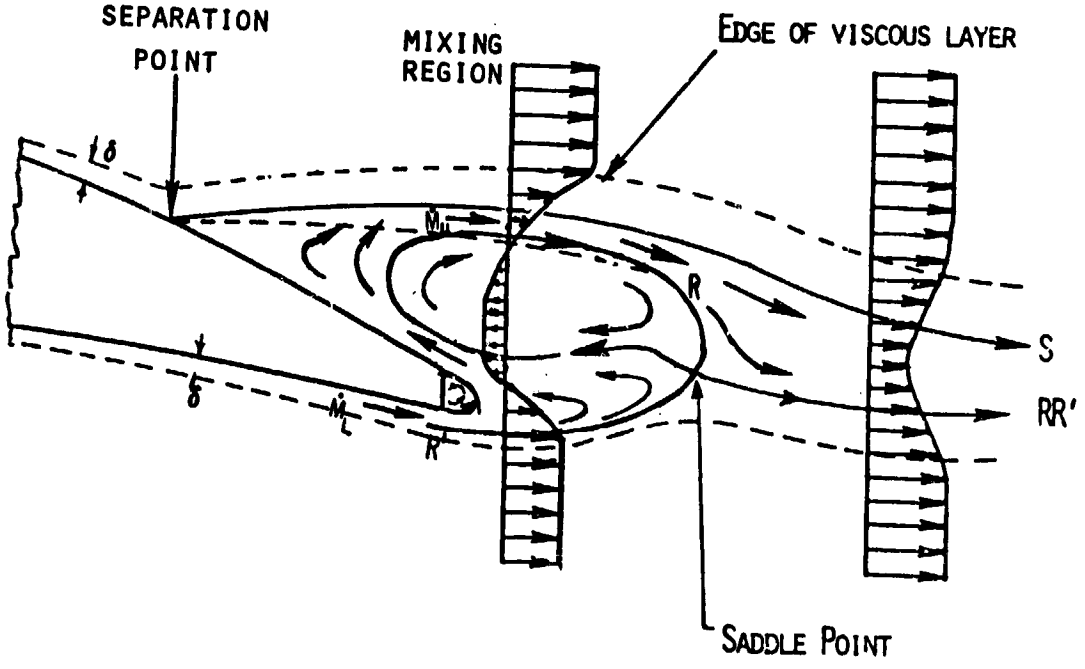

Figure 6.- Details of the separated region.

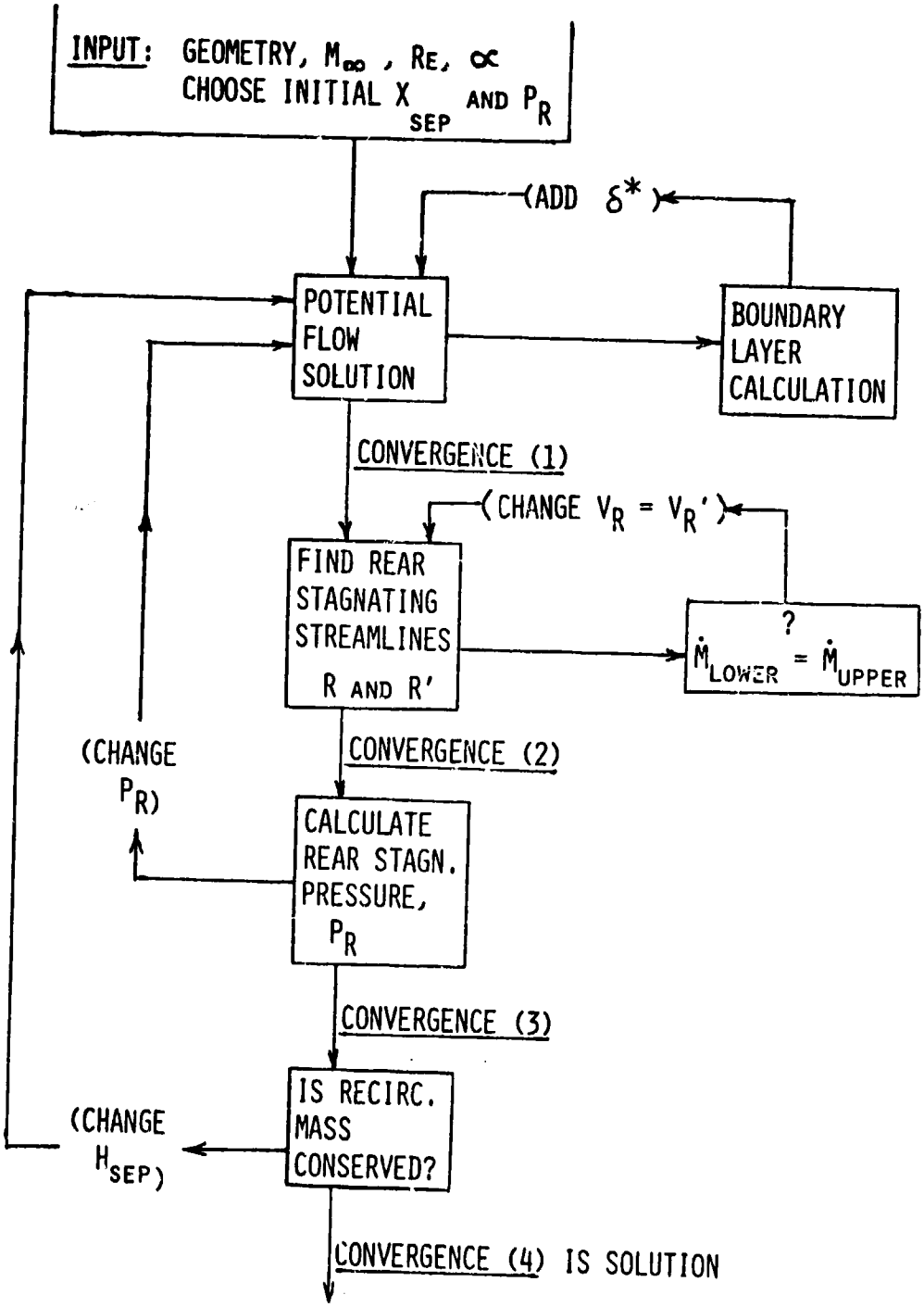

Figure 7.- Computer program logic.

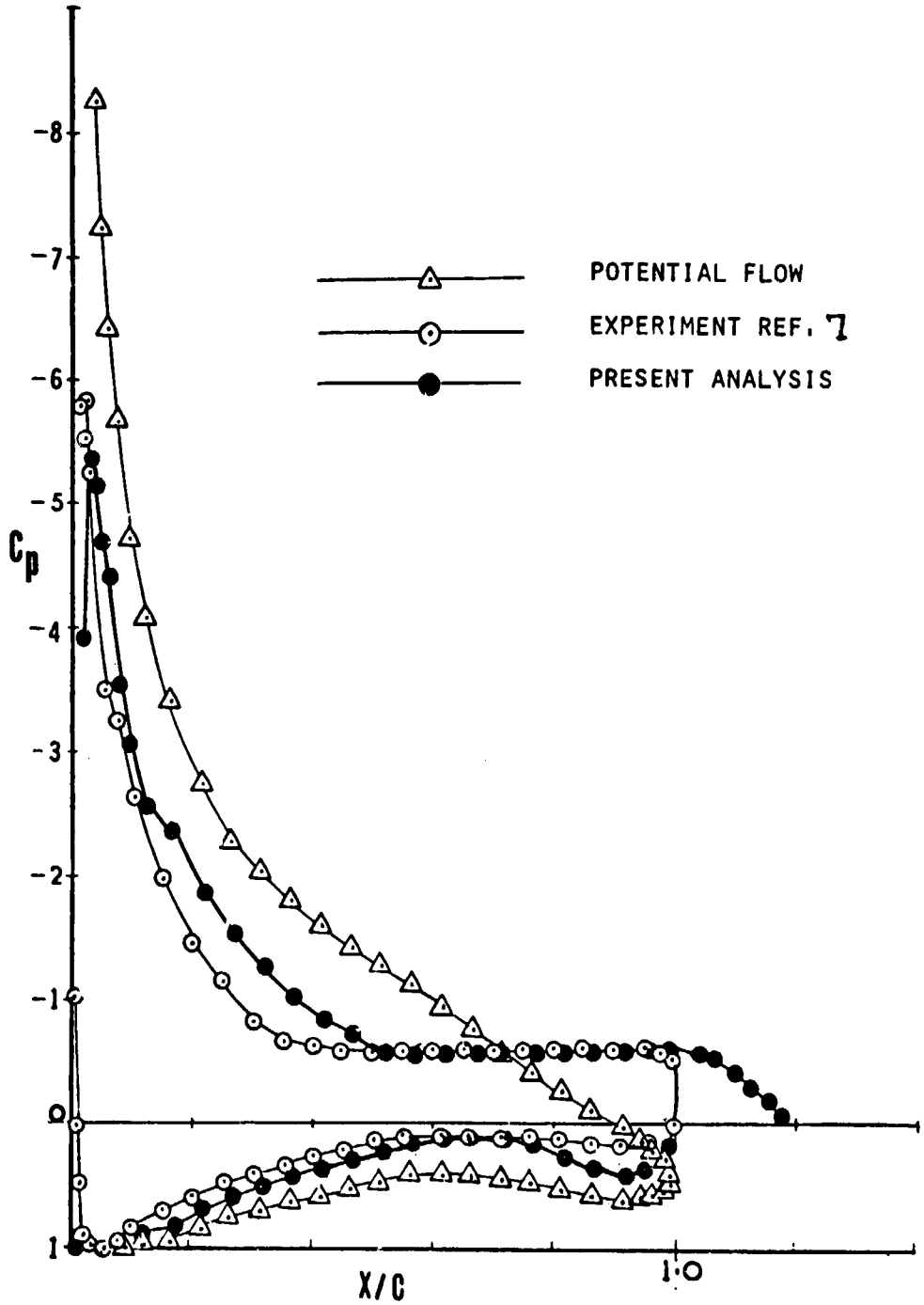

Figure 8.- Pressure distributions. GA(W)-1 airfoil. $\alpha = 18.4°$; R.N. = 2.5×10^6.

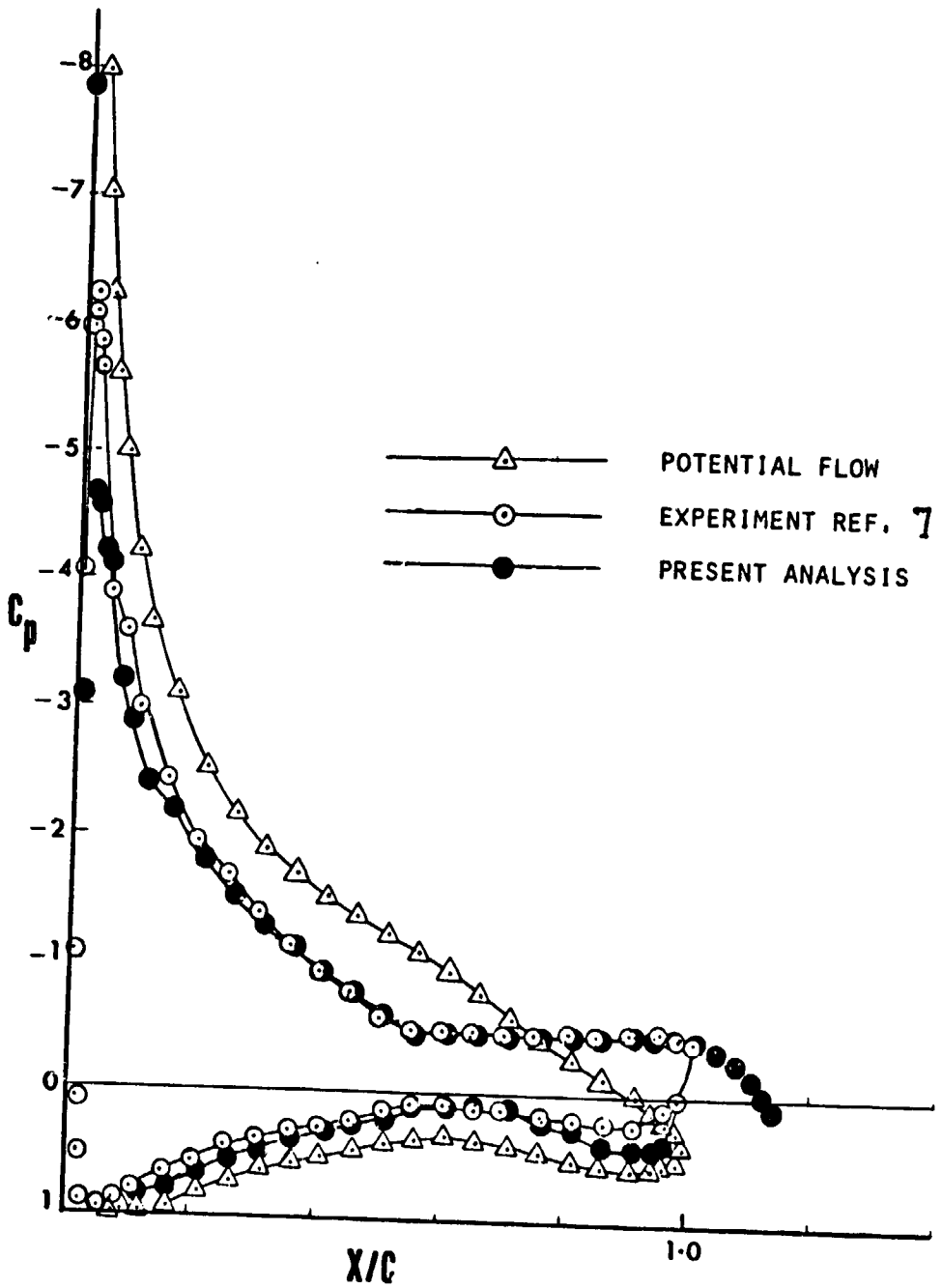

Figure 9.- Pressure distributions. GA(W)-1 airfoil.
$\alpha = 16.4°$; R.N. = 2.9×10^6.

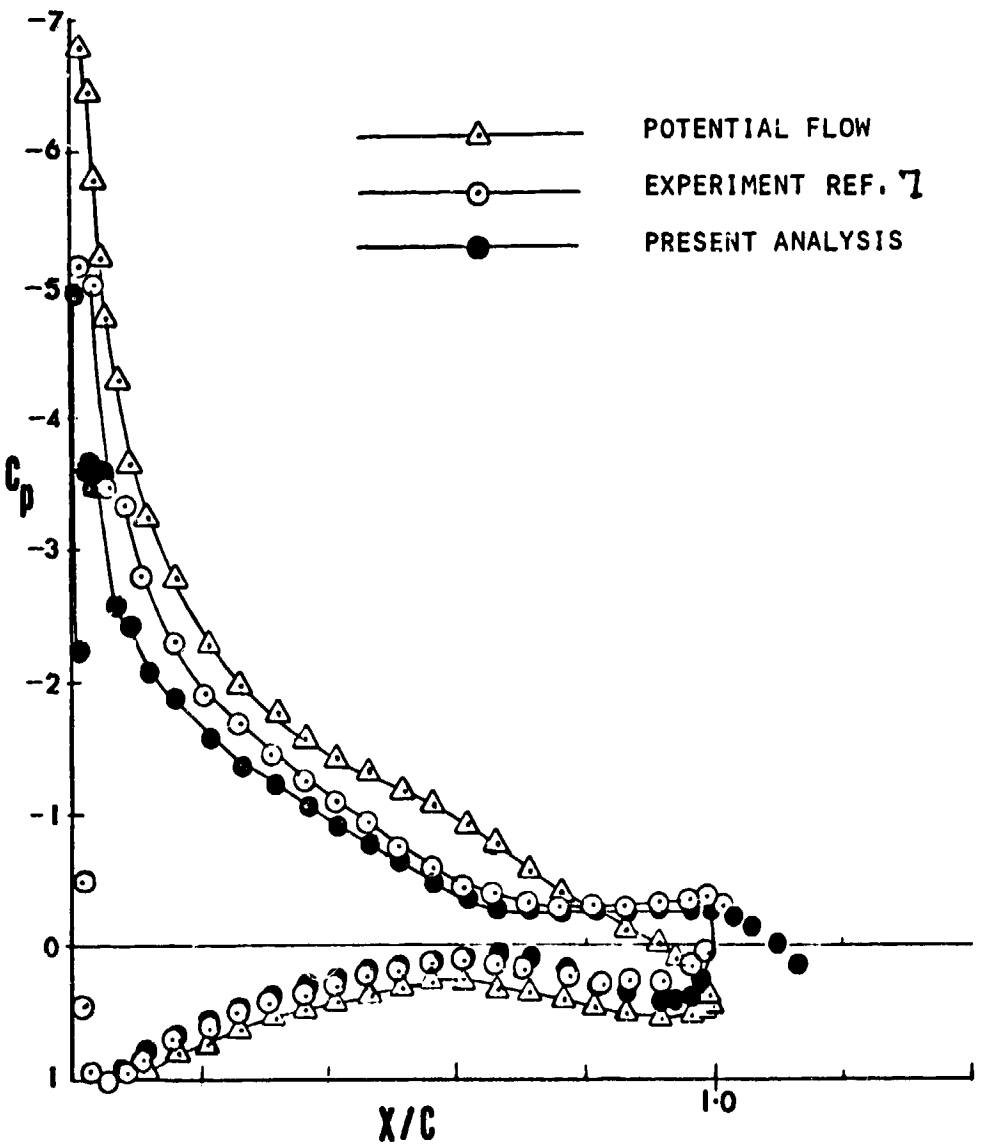

Figure 10.- Pressure distributions. GA(W)-1 airfoil. $\alpha = 14.4°$; R.N. = 2.9×10^6.